eNeuro

Research Article: New Research | Disorders of the Nervous System

Astrogliosis induced by brain injury is regulated by Sema4B phosphorylation

Sema4B regulates brain injury-induced astrogliosis

Liat Ben-Gigi[1,*], Sahar Sweetat[1,*], Elazar Besser[1], Yakov Fellig[2], Thorsten Wiederhold[3], Roberto D. Polakiewicz[3] and Oded Behar[1]

[1]*Department of Developmental Biology and Cancer Research, Institute of Medical Research Israel-Canada (IMRIC)], Faculty of Medicine, The Hebrew University, P.O. Box 12272, 91120 Jerusalem, Israel*

[2]*Neuropathology Unit, Department of Pathology, Hadassah–Hebrew University Medical Center, Jerusalem, Israel*

[3]*Cell Signaling Technology, Inc. 3 Trask Lane, Danvers, Massachusetts 01923, USA.*

DOI: 10.1523/ENEURO.0078-14.2015

Received: 29 December 2014

Revised: 6 May 2015

Accepted: 8 May 2015

Published: 18 May 2015

Author Contributions: LB-G, SS, and EB Performed Research, YF analyzed data, RDB and TW contributed unpublished reagents and OB designed research and wrote the paper.

Funding: The Legacy Heritage Biomedical Science Partnership: 1306/10. Israel Science Foundation: 947/14.

Conflict of Interest: Authors report no conflict of interest

*Contributed equally to this paper.

Correspondence should be addressed to Oded Behar, Email: odedb@ekmd.huji.ac.il.

Cite as: eNeuro 2015; 10.1523/ENEURO.0078-14.2015

eNeuro

http://eneuro.msubmit.net

eN-NWR-0078-14R2

Astrogliosis induced by brain injury is regulated by Sema4B phosphorylation

1) Manuscript Title: Astrogliosis induced by brain injury is regulated by Sema4B phosphorylation

2) Abbreviated Title: Sema4B regulates brain injury-induced astrogliosis

3) List all Author: Liat Ben-Gigi[1*], Sahar Sweetat[1*], Elazar Besser[1], Yakov Fellig[2] Thorsten Wiederhold[3], Roberto D. Polakiewicz[3] and Oded Behar[1#]

[1]Department of Developmental Biology and Cancer Research, Institute of Medical Research Israel-Canada (IMRIC)], Faculty of Medicine, The Hebrew University, P.O. Box 12272, 91120 Jerusalem, Israel. [2]Neuropathology Unit, Department of Pathology, Hadassah–Hebrew University Medical Center, Jerusalem, Israel. [3]Cell Signaling Technology, Inc. 3 Trask Lane, Danvers, Massachusetts 01923, USA.

[*] Contributed equally to this paper.

4) Author Contributions: LB-G, SS, and EB Performed Research, YF analyzed data, RDB and TW contributed unpublished reagents and OB designed research and wrote the paper.

5) [#]Correspondence should be addressed to OB (odedb@ekmd.huji.ac.il)

6) Number of Figures: 7

7) Number of Tables: 1

8) Number of Multimedia: 0

9) Number of words for Abstract: 130

10) Number of words for Significance: 116

11) Number of words for Introduction: 435

12) Number of words for Discussion: 1493

13) Acknowledgements: We thank Dr. Norman Grover (Department of Developmental Biology and Cancer Research, The Hebrew University) for helpful advice regarding the statistical analyses.

14) Conflict of Interest: Authors report no conflict of interest

15) Funding sources: This work was supported by a grant from Legacy Heritage Biomedical Science Partnership (Grant No. 1306/10) and by the Israel Science Foundation Grant No. 947/14)

Abstract:

Injury to the central nervous system (CNS) induces astrogliosis, an astrocyte-mediated response that has both beneficial and detrimental impact on surrounding neural and non-neural cells. The precise signaling events underlying astrogliosis are not fully characterized. Here, we show that astrocyte activation was altered and proliferation was reduced in Semaphorin 4B (Sema4B)-deficient mice following injury. Proliferation of cultured Sema4B$^{-/-}$ astrocytes was also significantly reduced. In contrast to its expected role as a ligand, the Sema4B ectodomain was not able to rescue Sema4B$^{-/-}$ astrocyte proliferation but instead acted as an antagonist against Sema4B$^{+/-}$ astrocytes. Furthermore, the effects of Sema4B on astrocyte proliferation were dependent on phosphorylation of the intracellular domain at Ser825. Our results suggest that Sema4B functions as an astrocyte receptor, defining a novel signaling pathway that regulates astrogliosis after CNS injury.

Significance Statement:

Astrocyte activation plays a critical role in response to CNS trauma. Following CNS injury, astrogliosis has the beneficial effect of restricting tissue damage, but it also limits neuronal regeneration. That modulation of astrogliosis may improve neuronal regeneration is a widely held view. However, the cellular and molecular mechanisms underlying astrogliosis are not fully characterized.

Here, we identify the involvement of an unexpected protein, Sema4B, a transmembrane member of the semaphorin family of proteins, in modulating astrocyte activation and proliferation in the aftermath of CNS injury. Although to date Sema4B has been shown to function as a ligand, our present results in astrocytes are more consistent with its function as a receptor or as a signaling molecule.

Introduction:

Brain damage as a result of stroke or head trauma is one of the leading causes of disability and death in humans. Brain trauma activates astrocytes in a process called reactive astrogliosis, which initiates changes in molecular expression and morphology and, in severe cases, scar formation (Sofroniew and Vinters, 2010). Although astrogliosis typically occurs in response to many types of insults, recent studies have demonstrated clear differences in gene-expression profiles between astrocytes activated by inflammation and by ischemic stroke (Zamanian et al., 2012). The overall effect of reactive astrocytes on injury outcome is not entirely clear, although accumulating evidence indicates that it may have both positive and negative consequences. Experimental ablation of astrocytes slows recovery from CNS injury, implying that the presence of reactive astrocytes is crucial under such conditions (Bush et al., 1999; Faulkner et al., 2004). However, the effect of astrogliosis on post-injury events may differ according to the specific signaling molecules involved. For example, deletion of STAT3 in astrocytes results in increased neuronal death and reduced recovery following CNS injury (Okada et al., 2006; Herrmann et al., 2008), whereas inhibition of NF-κB in astrocytes improves recovery (Brambilla et al., 2005). It thus appears that distinct signaling cascades specifically influence astroglial function to determine the outcome of brain pathology and the degree of neurological damage.

Upon injury, the astroglial response is evoked by several changes occurring in the CNS parenchyma. A variety of signals are produced, including cytokines and growth factors such as Sonic Hedgehog and epidermal growth factor (EGF) (Amankulor et al., 2009; Codeluppi et al., 2009). Although astrogliosis can potentially be triggered by any of these signals, the glial response itself is highly diverse and may

thus evoke additional signaling receptors and ligands. Since post-injury astrocytic borders and cell proliferation must be coordinated among the migrating and proliferating astrocytes, transmembrane ligand−receptor sets may serve as efficient mediators for communicating and coordinating this complex response. Members of the semaphorin family are good candidates for such functions. Some members of this gene family commonly act as ligands that bind directly to plexins (Pasterkamp, 2012). However, they may also operate in a reverse-signaling mechanism as receptors, as shown for Sema6D/PlexinA1 (Toyofuku et al., 2004). Semaphorins are up-regulated after injury, and numerous studies have shown that they regulate both cell proliferation and cell migration, making them intriguing candidates for post-injury astrocyte regulation (Pasterkamp and Verhaagen, 2006).

Because of its expression in astrocytes, Sema4B, a type 4 transmembrane semaphorin, is of particular interest in this context (Cahoy et al., 2008; Maier et al., 2011). Here, we examined the role of Sema4B in astrogliosis following brain injury.

Materials and Methods:

Antibodies, growth factors and materials. EGF was obtained from Peprotech. Anti-Iba1 was obtained from Wako. Anti-S100β was obtained from Abcam and from DAKO, Anti-*β-gal* was obtained from Abcam. Anti-GFAP, anti-phospho-Sema4B, anti-Sema4B, anti-vimentin, anti-tubulin α/β, anti-p-ERK1/2, anti-Ki-67, anti-myc and anti-NeuN were purchased from Cell Signaling Technologies (Danvers, MA). Anti-BrdU (G3G4, developed by S.J. Kaufman, was obtained from the Developmental Studies Hybridoma Bank developed under the auspices of the NICHD and maintained at the University of Iowa, Department of Biological Sciences, Iowa City, IA 52242, USA). BRDU flow kit was purchased from (BD Biosciences, San

Jose, CA, USA). Secondary antibodies were obtained from Jackson ImmunoResearch Laboratories (West Grove, PA, USA). All other reagents were purchased from Sigma (St. Louis, MO, USA).

Animals and surgical procedures. Sema4B$^{+/-}$ mutant mice were purchased from the Mutant Mouse Regional Resource Center (MMRRC). This mouse line was generated as a result of targeted trap alleles. In this mouse line Sema4B is retained within the intracellular compartment (Friedel et al., 2005). A heterozygous breeding strategy was adopted in order to obtain both wild-type, heterozygous (Sema4B$^{+/-}$) and mutant (Sema4B$^{-/-}$) mice. Both sexes were used in the experiments. All animal procedures were performed according to the regulations of the authors' university animal care committee.

All cortical injury experiments were performed on mice aged 7−8 weeks old. Genotype was determined by PCR analysis of genomic DNA isolated from tail clippings of 3-week-old mice. Presence of the wild-type Sema4B allele was established using primer 1 (5'-AGACATGGTGCTGGAGAGGT-3') with primer 2 (5'-TGTGTTTGGTTGGATCTGGA-3'). The mutant allele of Sema4B$^{-/-}$ was verified with primer 3 (5'-TGCACATGCTTTACGTGTG-3') and primer 4 (5'-TGCCGCGTGTCGTGTTGCAC-3').

For the injury experiments mice were anesthetized with ketamine/xylazine solution (50 mg/kg ketamine/7.5 mg/kg xylazine in 0.9% NaCl solution). A sterile needle was inserted vertically into the right cerebral hemisphere, reaching the skull surface at a depth of 5 mm. The needle was inserted through the cranium 2 mm caudal to the bregma and 1 mm lateral to the midline. The skin incision was closed with sutures.

Assays

Immunoblots. Astrocyte cultures (or tissue biopsy of the injury site) were harvested in lysis buffer (1% NP40, 0.5% sodium deoxycholate, 0.1% SDS, 150 mM NaCl, 10 mM buffered phosphate pH 7.2, 2 mM EDTA, 50 mM NaF, 0.2 mM orthovanadate and protease inhibitor cocktail). Cells were collected with a cell scraper, passed six times through a pipette tip, vortexed and incubated on ice for 15 min. The lysates were then centrifuged at 20,000 x g for 15 min and pellets were discarded. Protein concentration of each sample was determined using Bradford Reagent (Sigma). Samples containing 20 mg protein were boiled in 1 x SDS sample buffer, separated by SDS-10% polyacrylamide gel electrophoresis (PAGE) and blotted onto PVDF membranes (Millipore). The membranes were incubated in 5% fat-free milk in TBST (10 mM Tris-HCL pH 7.4, 150 mM NaCl, 0.1% Tween 20) for 1 h and then 5% BSA in TBST containing various dilutions of primary antibodies for 18 h at 4°C. The membranes were washed three times with TBST for 5 min each before and after incubation with secondary antibody. The proteins were detected with an appropriate secondary antibody (1 h, RT) coupled to horseradish peroxidase-conjugated goat anti-rabbit or anti-mouse antibody and visualized by chemiluminescence according to the manufacturer's instructions (West Pico, Pierce).

Bromodeoxyuridine injection. Bromodeoxyuridine (BrdU; Sigma, St. Louis, MO) was dissolved in 0.9% NaCl at a concentration of 10 µg/µL. For labeling of dividing cells, the injured mice received injections of BrdU (50 mg/kg body weight, i.p.) on days 3, 5 and 7 after injury. Mice were killed 3 h after the final injection, 7 days post-injury.

qPCR analysis. Total RNA (500 ng) in a total volume of 20 µL was reverse-transcribed with the ImProm-II™ Reverse Transcriptase cDNA Synthesis Kit

(Promega, Madison, WI) according to the manufacturer's instructions. The resulting cDNA reaction mix was then diluted 20 times in double-distilled water. Real-time quantitative PCR (qPCR) was performed with the SYBR Green mix (Roche) according to the manufacturer's instructions.

The specific primers were as follows:

Sema4B primers, forward: 5'-GTGGGACGTAACTCCTTCCA-3';

reverse: 5'-AGGTTGCTCAAGTGGAATCG-3';

GAPDH primers, forward: 5'-TCAATGAAGGGGTCGTTGAT-3';

reverse: 5'-CGTCCCGTAGACAAAATGGT-3';

ALDH1L1, forward: 5'-GACAAGGATGGGAAAGCAGA-3';

reverse: 5'-CCACCGAGGGAACTTAAACA-3';

GFAP, forward: 5'-CAGCCTCAGGTTGGTTTCAT-3';

reverse: 5'-GGAGAGGGACAACTTTGCAC-3';

Vimentin primers, forward: 5'-GAAATTGCAGGAGGAGATGC-3';

reverse: 5'-GTGCCAGAGAAGCATTGTCA-3'.

LCN-2 primers, forward: 5'-CCTGGAGCTTGGAACAAATG-3'

reverse: 5'-ATGTCACCTCCATCCTGGTC-3'

Amplicon purity and size were verified by melt-curve analysis and gel electrophoresis. Each sample was normalized relative to GAPDH and ALDH1L1 with similar results.

Immunofluorescence analysis. Brains were fixed in 4% paraformaldehyde, following by incubation in 30% sucrose for at least 24 h. Tissue sections (25 micrometers thick) were incubated for 1 h in a blocking solution consisting of 0.3% Triton X-100, and 5% goat serum. This solution was used for the dilution of both primary and secondary antibodies. Sections were incubated in the primary antibody overnight (16 h). Slides

were then washed three times (5 min each) with PBS and visualized with Cy3- and Cy5-labeled secondary antibodies and coverslipped. Every 5th section was stained and analyzed with the different antibodies. At least seven sections were analyzed for each mouse. Each section was analyzed by confocal microscopy in 5 µm optical sections, and the non-injured side was used to determine background levels.

Sections were analyzed using a laser-scanning confocal microscope (FV1000; Olympus). Z-stack images were acquired with a ×20 objective, 0.5 µm steps, and confocal acquisition software (FluoView, Olympus, Hamburg, Germany).

Sema4B knockdown. For Sema4B knockdown experiments we used MISSION® shRNA lentiviral vectors. For mouse Sema4B we used TRCN0000112290 (shRNA1) and TRCN0000112293 (shRNA2). Non-target shRNA (sh-scramble) was used as a control.

Lentivectors and lentiviral preparation. The cDNA encoding mSema4B was mutated to replace amino acids 666-673 (MDQK*NQ*RD) with the myc tag sequence (MEQKLISEE DL). This location has low conservation between mice and humans. It is located between the Ig domain and the transmembrane domain. This myc tag Sema4B was also mutated to generate cDNA encoding Sema4B in which Ser825 was replaced by alanine (S825A) or aspartic acid (S825D). All three alternative forms of Sema4B were cloned into a pLenti6.2 vector and co-transfected into HEK293 cells with expression vectors containing all the genetic elements required for pseudoviral particles. The titers of the different viruses used in rescue experiments were measured.

Fusion Proteins. The Fc fusion protein of the ectodomain of mouse Sema4B (amino

223 acid 1-700) was cloned into PsxFc2 vector upstream of the hinge region of human
224 IgG1-Fc. Fc protein was used as control. Fusion proteins were transiently expressed
225 in 293 cells and were collected 72 h later. Concentrations of the Fc fusion proteins
226 were evaluated by western blot with anti-hIgG antibody.

227 **Astrocyte cell culture.** Mouse primary cortical astrocytes were cultured essentially as
228 described previously, with minor modifications (Schildge et al., 2013). Briefly,
229 cerebral hemispheres were aseptically removed from newborn (2-day-old) pups and
230 the cortices were incubated in 0.25% trypsin for 10 min at 37°C. Tissues were then
231 mechanically dissociated and resuspended in Dulbecco's modified Eagle's medium
232 (DMEM) containing 15% fetal bovine serum (FBS) and antibiotics. Cells were grown
233 in pre-coated poly-L-lysine 140 cm^2 culture plates in DMEM with 10% FBS for three
234 days. The medium was replaced on day 3 with modified DMEM (with D-valine
235 instead of L-valine) and dialyzed serum. The new selection medium did not support
236 growth of fibroblasts and inhibited their proliferation. Astrocytes reached confluence
237 between day 7 and day 10. Each culture preparation was tested for astrocyte purity by
238 staining with anti-S100β. All cultures were between 98% and 100% positive for this
239 marker.

240 **Adult astrocyte isolation.** Cortices of a few adult mice were dissected and
241 dissociated using papain and DNase as described (Moussaud and Draheim, 2010).
242 Astrocytes were then purified using anti-GLAST MicroBeads (Miltenyi Biotec)
243 according to the manufacturer's protocol and protein was immediately extracted to be
244 used in western blot analysis.

Flow cytometry of adult astrocytes. A biopsy of 3x3 mm around the site of injury in the cortex was removed 7 days following injury and PBS perfusion and dissociated using papain. The cells were stained with anti-GLAST and anti-BrdU and analyzed by flow cytometry (MACSQuant Analyzers, Miltenyi Biotec, Cambridge MA, USA).

Statistical analysis. Values presented are mean ± s.e.m. A p value < 0.05 was considered significant. Statistical analysis was performed using one-tailed or two-tailed Mann–Whitney test. Where relevant, *P*-values were adjusted for multiple comparisons in accordance with the Bonferroni procedure; overall *P*-values for the different injury experiments were then computed from these adjusted *P*-values using Fisher's chi-square test for combined probabilities. Symbols are as follows: *P<0.05, **P<0.001, ***P<0.0001.

Results:

Sema4B is expressed in injured adult cortex astrocytes

We employed a cortical stab-wound lesion model to investigate the possible role of Sema4B in brain injury. We first decided to map the types of cells expressing Sema4B in the cortex using a secretory trap mouse (Friedel et al., 2005). The β-galactosidase (β-gal) reporter gene in this mouse was fused to Sema4B (forming a Sema4B-β-gal chimeric protein which is retained within an intracellular compartment). Immunofluorescence staining was used to analyze heterozygous Sema4B mice for β-gal reporter expression *in vivo*. We examined the cortex before, and 1, 3 and 7 days following, stab-wound injury, and at different distances from the site of injury, to include all cell types which may express Sema4B as a result of the injury. We co-stained for the β-gal reporter (which recognizes the Sema4B fusion protein), GFAP (for glial fibrillary acid protein, an astrocyte marker) and NeuN (a neuronal marker), using specific antibodies. We also co-stained for the β-gal reporter,

GFAP and Iba1 (microglia marker). For each cell type and for each time point we monitored hundreds of cells in different sections prepared from three different mice. Sema4B was never detected together with NeuN or Iba1 in any of the β-gal-positive cells (Fig. 1a). In contrast, most β-gal-positive cells (at days 3 and 7) were also GFAP-positive, indicating that in the mouse cortex, Sema4B is mostly expressed by astrocytes. To quantify this observation we counted the number of β-gal-positive and GFAP-positive cells seven days after injury (Fig. 1b). Most GFAP-positive cells (about 90%) are also β-gal-positive; GFAP-positive staining was undetectable in only 5.6% of the β-gal-positive cells. These cells may still be astrocytes, but with low or no detectable levels of GFAP expression.

We also looked for alternative methods to identify the types of cells expressing Sema4B. We tested a number of commercially available antibodies raised against Sema4B. None of the antibodies were useful in immunohistochemistry, but one of the antibodies worked well in western blots. We validated this antibody using $Sema4B^{+/+}$ and $Sema4B^{-/-}$ brain lysates (Fig. 1c). Sema4B was detected in wild-type mice at its expected size (about 110 kD; an additional non-specific band just above this band was also detected). In $Sema4B^{-/-}$ mice Sema4B was detected at a size of about 190 kD, corresponding to the expected size of the Sema4B-β-gal fusion protein. We therefore used this antibody to confirm the types of cells expressing Sema4B. We first isolated astrocytes from mice cortices using an anti-EAAT1/GluT-1/GLAST (ACSA-2)-magnetic cell separation kit. Using ACSA-2-APC-labeled antibody in FACS analysis, we determined that the positive astrocyte fraction consisted of at least 75% astrocytes, while the negative fraction included only 8% astrocytes (Fig. 1d). This is likely to be an underestimate of the GLAST-bearing cells in the positive fraction since the ACSA-2 beads may reduce the efficiency of ACSA-2-APC binding during the FACS

analysis. We then evaluated both negative and positive cell populations by western blotting. The proteins extracted from these cell populations were tested with antibodies against Sema4B and tubulin (Fig. 1e). Sema4B was detected in the astrocyte fraction, but not in the non-astrocyte fraction of cells, indicating that Sema4B expression in the cortex is restricted to the astrocyte cell population.

Astrocyte activation is modified in Sema4B$^{-/-}$ mutant mice

To investigate a possible role of Sema4B in astrogliosis we analyzed cortical stab-wound lesions of adult Sema4B$^{-/-}$ mutants and their littermates (Sema4B$^{+/-}$ and Sema4B$^{+/-}$ or Sema4B$^{+/+}$). We focused on day 7 post-injury, by which activation of astrogliosis is known to reach its peak (Robel et al., 2011).

A hallmark of astrocyte activation is up-regulation of GFAP (Kindy et al., 1992; Yamashita et al., 1996). Expression of GFAP in astrocytes of the intact adult mouse cortex is very low in the absence of astrogliosis, but is significantly increased after CNS injury (Kindy et al., 1992; Yamashita et al., 1996). To monitor the activation of astrocytes we first tested the expression of GFAP by immunofluorescence staining. Staining of horizontal cortical sections from unilaterally injured Sema4B mice revealed elevated GFAP levels almost exclusively on the injured side (both Sema4B$^{+/+}$ and Sema4B$^{+/-}$ were indistinguishable). Strong astrocyte staining was also observed around the stab-wound site, with GFAP-positive processes extruding from astrocytes to form the astroglial barrier. GFAP staining of the Sema4B$^{-/-}$ mutant mice, though present, was significantly reduced (Fig. 2a). This reduced GFAP activation can be the result either of limited GFAP activation or reduced astrocyte number. To address this point we stained Sema4B$^{+/-}$ and Sema4B$^{-/-}$ mice cortices with or without injury with x-gal (Fig. 2b). We tested the cell density of x-gal (Sema4B-positive/mm^2), comparing Sema4B$^{+/-}$ and Sema4B$^{-/-}$ mice cortices without injury.

There was no significant difference in x-gal-positive cell density between genotypes, indicating that Sema4B-expressing astrocytes (in Sema4B$^{+/-}$ mice) are not lost in Sema4B$^{-/-}$ mice (Fig. 2c). We also tested the density of x-gal-positive cells in both Sema4B$^{+/-}$ and Sema4B$^{-/-}$ mice cortices after injury. Again, no significant difference between the two genotypes after injury was detected (Fig. 2d). We then stained for S100β, another astrocyte marker, and tested the density of cells with or without injury (Fig. 2e). Again, no significant change in the number of S100β cells was detected (Fig. 2f,g), demonstrating that the lack of GFAP activation is not the result of a reduced number of astrocytes (we did not try to co-localize the x-gal and the S100β since the conditions of the two methods are incompatible).

Real-time PCR was employed to assay *GFAP* expression in mRNA extracted from cortical tissue around the stab wound to obtain more quantitative information on astrocyte activation levels. *GFAP* expression in the non-injured brains of Sema4B$^{+/-}$ and Sema4B$^{-/-}$ mutant mice was similar. In contrast, expression of *GFAP* mRNA in Sema4B$^{-/-}$ seven days after stab-wound injury was about 2.5-fold lower than in the Sema4B$^{+/-}$ mice (Fig. 2B). To test if GFAP is the only gene affected in Sema4B$^{-/-}$ mice, we also tested the expression of two additional markers of astrocyte activation (vimentin and Lipocalin-2 (LCN-2)). Vimentin, another intermediate filament protein which is induced by some reactive astrocytes (Galou et al., 1996), was increased to the same extent in the injured cortices of the Sema4B$^{+/-}$ and Sema4B$^{-/-}$ mutant mice (Fig. 2i). In contrast, LCN2, an iron-trafficking protein shown to be specifically induced in astrocytes following inflammation and stroke (Zamanian et al., 2012), was also induced following stab-wound injury, but activation in Sema4B$^{-/-}$ mice was about 1.5 times higher compared to Sema4B$^{+/-}$ mice (Fig. 2j). These results suggest that astrocytes are activated following cortical injury in

Sema4B$^{-/-}$ mice, although their activation profile differs from that of wild-type astrocytes.

Astrocyte proliferation is reduced in Sema4B mutant astrocytes *in vivo*

A restricted number of astrocytes proliferate in response to cortical injury (Bardehle et al., 2013). To monitor the effect of Sema4B on injury-induced proliferation, we injected Sema4B$^{-/-}$ mutant mice and wild-type littermates with BrdU, a marker of cell proliferation, on post-injury days 3, 5 and 7, a strategy that ensures that most of the proliferating cells will be labeled (cell counts on day 7 are shown in Fig. 3). There were significantly fewer BrdU-positive cells per section area near the site of injury (indicating significantly less cell proliferation) in the Sema4B null mice than in the wild-type mice (Fig. 3B). There was an even greater percentage reduction in the BrdU-positive cells that were also positive for GFAP in the mutant mice than in the wild-type mice (Fig. 3c), suggesting that most of the cells that exhibited a decreased rate of proliferation in the absence of Sema4B were astrocytes.

We cannot, however, rule out that the observed difference between the total cell count and the GFAP-positive cell count is not simply because GFAP immunostaining is reduced in the Sema4B mutant mice. To test the proliferation of astrocytes in a manner independent of GFAP, and to overcome the limitation of immunohistochemistry, we also tested proliferation using flow cytometry analysis. In these experiments, the astrocytes were labeled with anti-GLST and anti BrdU (again injected on days 3, 5 and 7). Consistent with the immunostaining experiments, we detected a reduction in total cell proliferation and specifically astrocyte proliferation. Although reduction in astrocyte proliferation significantly contributes to the reduction in cell proliferation, it is possible that other, as yet unidentified, cell type(s) are less proliferative after injury in the cortices of Sema4B$^{-/-}$ mice.

Proliferation of Sema4B$^{-/-}$ astrocytes *in vitro* is reduced

To further investigate the role of Sema4B in astrocytes under more controlled conditions, we measured astrocyte proliferation *in vitro*. As a first step, we tested whether Sema4B is expressed by astrocytes in culture. As shown in the cortex, astrocytes obtained from Sema4B$^{+/-}$ mice are also positive for β-gal (Fig. 4a). After confirming that Sema4B is expressed by astrocytes in culture, we compared the proliferation of Sema4B$^{+/-}$ and null astrocytes *in vitro*. Astrocytes were serum-starved for three days, and then stimulated with serum for 16 h. Staining of the cells with Ki-67 antigen, a marker of cell proliferation, clearly showed that astrocytes from Sema4B-deficient mice are less responsive to serum-induced proliferation than those from the heterozygous control (Fig. 4b).

To exclude the possibility that the effect on astrocyte activation in the Sema4B mutant astrocytes is caused either by gain-of-function by the fusion protein (Sema4B-β-gal) or because a pre-established developmental defect underlies the abnormal response of Sema4B$^{-/-}$ astrocytes, we acutely inhibited Sema4B expression by infecting wild-type primary astrocytes with two different shRNAs targeting Sema4B. Both shRNAs reduced the protein levels of Sema4B to almost undetectable levels compared to scrambled shRNA (Fig. 4c). As in the case of astrocytes from Sema4B$^{-/-}$ mutant mice, shRNA knockdown of Sema4B expression also reduced cell proliferation (Fig. 4d). To validate the shRNA experiment we carried out a rescue experiment in which we infected astrocytes with both Sema4B expression vector and shRNA targeting Sema4B. Unfortunately, validation of our shRNA experiments was not possible since astrocytes were not viable after selection for both viruses, probably because the infection efficiency was not high enough. Nevertheless, since both the

shRNA and the Sema4B mutant astrocytes show very similar results, it is most likely that Sema4B is indeed required for astrocyte proliferation.

Sema4B expression is not regulated at the level of mRNA or protein expression

Our results thus far indicate that Sema4B is needed for astrocyte activation and proliferation following injury. It is therefore possible that Sema4B expression would be increased following injury. We first tested whether Sema4B is regulated at the level of mRNA expression by measuring the levels of Sema4B mRNA at different time points after cortical injury (Fig. 5a). The results indicated that Sema4B is not regulated at the level of mRNA, prompting us to study whether Sema4B may be regulated at the protein level. To test this possibility, we extracted proteins from cortical biopsies of the site of injury at different time points. The protein levels of Sema4B were also not significantly changed (Fig. 5b). Finally, we did not detect any changes in the protein levels of Sema4B in astrocytes in response to *in vitro* injury (Fig. 5c). Although globally Sema4B does not appear to be regulated by injury, it is still possible that Sema4B is up-regulated in some cells in the cortex, while in other cells it is down-regulated. However, histochemical staining with x-gal (Fig. 2b) does not support this possibility. Thus, Sema4B is neither regulated at the RNA nor the protein level following injury.

Sema4B is phosphorylated at S825 following injury or growth factor stimulation

Although we have not detected injury-related regulation of Sema4B expression, our genetic evidence indicates that it has an important role in astrocyte activation after injury. We therefore considered the possibility that Sema4B is regulated post-translationally. An earlier study showed that Sema4B is phosphorylated at serine 825 in some cancer cell lines stimulated with growth factors such as EGF (Moritz et al., 2010). To examine whether Sema4B is phosphorylated after injury, we assayed

Sema4B phosphorylation at different times after cortical stab-wound injury in Sem4B$^{+/+}$ mice using a phosphorylation-specific antibody directed against serine 825 of Sema4B. First, the specificity of the antibody was tested using brain tissue from Sema4B$^{+/+}$ and Sema4B$^{-/-}$ mice. Since β-gal and a stop codon are inserted upstream to the transmembrane domain, we expected that phospho-Sema4B would not be present in mutant mice. Indeed, we found that the antibody is highly specific and identifies phospho-Sema4B only in wild-type mice (Fig. 6a). Using this antibody, we detected rapid phosphorylation of Sema4B, with a peak 1-5 h following stab-wound injury (Fig. 6b, c).

Astrocytes isolated *in vitro* were used to study this phosphorylation more carefully. A rapid increase in Sema4B phosphorylation was also detected in confluent primary astrocytes following a scratch wound (Fig. 6d, e). As a positive control, we monitored ERK1/2 phosphorylation, shown to be activated in scratch-wound experiments (Mandell et al., 2001). The kinetics of ERK1/2 and Sema4B phosphorylation was very similar. It has been shown in the past that EGFR is activated in astrocytes following injury and can affect astrocyte response (Yang et al., 2011). We therefore tested the effects of EGF on Sema4B phosphorylation. As in the model of injury, primary astrocytes stimulated with EGF were rapidly phosphorylated at this site (Fig. 6f, g). These results indicate that regulation of Sema4B may occur through phosphorylation at serine 825.

Sema4B does not function as a ligand in astrocyte proliferation

Although Sema4B phosphorylation is more consistent with a receptor or signaling molecule, semaphorins in general, and Sema4B in particular, are known to function as ligands. The best example for this is the activity of Sema4B in the immune system. In this system, the Sema4B ectodomain has been shown to be

necessary and sufficient to rescue the Sema4B$^{-/-}$ phenotype in the immune system (Nakagawa et al., 2011). To test whether Sema4B functions as a ligand in our system, we examined whether the ectodomains of Sema4B (Sema4B-Fc) can rescue the proliferation response of Sema4B$^{-/-}$ astrocytes to serum stimulation (Fig. 7a). Sema4B-Fc was not able to rescue the proliferation defect of astrocytes, implying that Sema4B may function as a receptor. If this were the case, we speculated that the ectodomains of Sema4B might act as a competitive inhibitor on wild-type astrocytes. To test this possibility, we repeated the same experiment, this time using wild-type astrocytes. Consistent with this idea, Sema4B-Fc reduced the serum-induced proliferation response (Fig. 7b). Based on these experiments, we considered the possibility that the intracellular domain of Sema4B is critical for its activity.

Sema4B phosphorylation at S825 is required for astrocyte proliferation

Since Sema4B undergoes rapid phosphorylation after injury or growth factor stimulation at the intracellular domain, we examined whether such phosphorylation is important for the activity of Sema4B. We generated lentiviral vectors expressing either wild-type (full-length) Sema4B or a phosphorylation-resistant Sema4B, in which serine 825 is mutated to alanine, Sema4B^{S825A}, as well as and Sema4B^{S825D}, a mutant form of Sema4B that probably mimics constitutive phosphorylation. We used the lentiviral vectors expressing either Sema4B mutant or wild-type proteins to infect astrocytes from Sema4B$^{+/-}$ and Sema4B$^{-/-}$ mice, and monitored cell proliferation by Ki-67 staining. To make sure that the mutations do not affect the expression or localization of Sema4B, we added a myc-tag to the extracellular domain of Sema4B (see details in the methods section) to monitor the level of protein expression as well as cellular localization. All three Sema4B vectors resulted in similar expression, as shown by western blots (Fig. 7c). To test whether Sema4B over-expression mutants

are present correctly on the membrane, we utilized the localization of the myc tag in the extracellular domain to monitor expression in the cells without detergent, assuming that the myc tag would not be detected inside the cells. To check this assumption, we transfected HEK293 cells with PlexinA1 that contains a myc tag at the intracellular domain of the protein. The cells were stained with (Fig. 7g) or without (Fig. 7d) detergent. The results show that in the absence of detergent, the cells are negative for myc tag. We then infected astrocytes with the different mutants and the empty vector, and stained the cells without detergent (Fig. 7e,f,h,i). The results clearly show that all Sema4B mutants are expressed correctly on the membranes of the astrocytes.

We subsequently used these vectors to test whether Sema4B function can be rescued in Sema4B mutant astrocytes. As shown in Figure 7j, the Sema4B^{S825A} mutant was not able to overcome the proliferation defect in Sema4B$^{-/-}$ mutant astrocytes. In contrast, cell proliferation was restored in Sema4B$^{-/-}$ mutant astrocytes expressing either the wild-type Sema4B or Sema4B^{S825D}.

Thus far, we have found that Sema4B is phosphorylated following injury and that it needs to be phosphorylated in order to be able to function. However, can the phosphorylated form of Sema4B bypass the need for serum stimulation in order for astrocytes to proliferate? To answer this question, the lentiviral vectors were used to infect wild-type astrocytes with either wild-type Sema4B or constitutive phosphorylation mutant Sema4B^{S825D} (Fig. 7k). As expected, astrocytes infected with Sema4B wild-type vector showed low proliferation levels in the absence of serum and proliferated readily when serum was added. In contrast, astrocytes infected with Sema4B^{S825D} were highly proliferative (at least based on their Ki67 levels)

493 independent of serum addition. This result suggests that phosphorylation of Sema4B
494 at serine 825 can bypass the need for serum-dependent astrocyte proliferation.
495
496 **Discussion**
497 Sema4B is a transmembrane type 4 semaphorin which has been suggested to be
498 expressed in astrocytes (Liu et al., 2006; Lovatt et al., 2007; Cahoy et al., 2008; Maier
499 et al., 2011); however, the role of the *Sema4B* gene in astrocytes following brain
500 injury is not known. Here, we show not only that astrocytes are likely the only cells in
501 the adult cortex that express Sema4B, but also that Sema4B is essential for post-injury
502 astrogliosis.
503 Cortical injury is known to induce expression of GFAP, a classic marker of
504 astrocyte identity and activation, as well as astrocyte cell proliferation. Post-injury
505 GFAP activation and astrocyte cell proliferation were significantly decreased in
506 Sema4B$^{-/-}$ mutant mice compared to wild-type mice. This is likely not indicative of
507 reduced astrocyte numbers since the density of S100β-positive cells as well as x-gal
508 (Sema4B)-positive cells did not differ significantly. This also does not appear to
509 reflect blocking of astrogliosis, since LCN2 and v*imentin*, other known markers of
510 reactive astrocytes (Zamanian et al., 2012), are induced in both Sema4B$^{-/-}$ and control
511 mice. These results suggest that Sema4B is part of a specific signaling pathway
512 required for astrocyte activation upon injury.
513 In this study we used a global Sema4B-β-gal gene trap. In wild-type cells, Sema4B is
514 located at the cell membrane. In contrast, in the Sema4B-β-gal gene trap, the chimeric
515 protein formed is retained within an intracellular compartment. Although the
516 expression of a chimeric protein in a new cellular localization may result in a gain of
517 function, our results do not support this possibility. First, we did not see any

difference between wild-type and heterozygous mice in any of the assays we tested, both *in vitro* and *in vivo*. Moreover, astrocyte proliferation is reduced in knockdown experiments, similar to the situation of astrocytes isolated from Sema4B mutant mice. Unfortunately, we were not able to verify the knockdown result with a rescue experiment, most likely due to technical difficulty. Nevertheless, although it is difficult to completely rule out the possibility that the shRNA result is somehow compromised, since a similar phenotype is observed in both mutant mice and shRNA Sema4B-treated astrocytes, this possibility is unlikely. Thus, the fusion protein is not likely to have a biological function.

An additional concern related to the use of this model is whether the effects on astrocyte activation we detected are a direct result of the mutation of Sema4B in astrocytes or in other cells. Although it is difficult to completely rule out the latter possibility, we do not think it is likely. First, we showed that in the cortex, Sema4B is most probably restricted to astrocytes and therefore, it is not likely that other cells are involved. In the context of the immune system, some T and B cells express Sema4B in the periphery (Nakagawa et al., 2011). Treatment with ectodomains of Sema4B represses secretion of IL-4 and IL-6 by immune cells, and activation of basophils in Sema4B-/- mice is increased (Nakagawa et al., 2011). Thus, it is theoretically possible that the function of Sema4B in the immune system influences indirectly the astrocyte response. It is not known whether T or B cells, which could enter the cortex after injury, also express Sema4B. There is a remote possibility that a small number of T or B cells expressing Sema4B enter the cortex. However, even if we missed a small number of Sema4B-expressing immune cells, it is not likely to be the reason for the reduced activation of GFAP or proliferation of astrocytes, since in Sema4B$^{-/-}$ mice IL-6 and IL-4 secretion and basophil activation are likely to be stronger. We would

543 therefore expect to see increased inflammation as well as increased GFAP expression.
544 Instead, we found that GFAP expression is reduced. Moreover, the number and
545 profile of the immune cells in the cortex are not changed (data not shown). Finally,
546 astrocytes *in vitro* show a similar phenotype to that of astrocytes *in vivo*. Thus, in the
547 context of stab-wound injury, it is almost certain that Sema4B expressed by astrocytes
548 affects them directly.

549 **Regulation of Sema4B during injury**

550 Sema4B does not appear to be regulated at the level of RNA or protein
551 following injury. Instead, we found that Sema4B was phosphorylated at Ser825
552 following injury *in vitro* and *in vivo*. Recent work identified Ser825 as a site of
553 Sema4B phosphorylation following mitogen stimulation in cancer cells (Moritz et al.,
554 2010). This phosphorylation site is embedded within a sequence motif containing
555 arginine residues at the 5' and 3' positions, typical of AGC kinases regulated by
556 mitogenic stimuli such as Akt, RSK and p70 S6K. Using Sema4B null astrocytes in
557 reconstitution experiments with Sema4B phosphorylation mutants, we found that
558 Sema4B phosphorylation is critical for serum-induced astrocyte proliferation.
559 Moreover, since constitutive phosphorylation mimic of Sema4B reduces the need for
560 serum-induced proliferation, it seems that phosphorylation of Sema4B is necessary
561 and sufficient for this type of proliferative signal in astrocytes.

562 Interestingly, the regulation of Sema4B phosphorylation shortly after injury
563 suggests that this protein is part of an early response of the astrocytes. Indeed, we see
564 an indication of this in the over-activation of LCN2 in mutant mice just 24 h after
565 injury. Nevertheless, most prominent markers of astrocyte activation, namely GFAP
566 activation and proliferation, are induced days later. It is therefore tempting to
567 speculate that Sema4B activity is needed to initiate a signaling cascade, which

568 triggers a modified astrocyte activation profile. A similar profile is also observed with
569 critical regulators of astrocyte activation such as Stat-3, which is phosphorylated
570 shortly after injury (peak between 3-6 hours after injury) (Oliva et al., 2012), while
571 the most dramatic effects on astrocyte activation are most prominent 7-14 days after
572 injury (Okada et al., 2006).

573 **How does Sema4B regulate astrocyte activation?**

574 Sema4B is a member of the semaphorin family, which comprises 20 evolutionarily
575 conserved proteins classified as secreted (type 3) or transmembrane (types 4–6)
576 (Pasterkamp, 2012). Semaphorins commonly act as ligands that bind directly to
577 plexins or neuropilins. For example, Sema4B negatively regulates basophil-mediated
578 immune responses (Nakagawa et al., 2011). The fact that the ectodomain of Sema4B
579 is sufficient for this effect on basophils provides evidence that Sema4B functions in
580 this system as a ligand. However, at least type 6 semaphorins may also operate in a
581 reverse-signaling mechanism as receptors, as shown for Sema6D/PlexinA1 (Toyofuku
582 et al., 2004). Thus, it is possible that transmembrane semaphorins such as Sema4B
583 may also function as receptors.

584 Does Sema4B function as a receptor or a ligand in modulating astrocyte
585 activation? The dependence of astrocyte activation on Sema4B, shown in this study,
586 as well as the fact that Sema4B is expressed in astrocytes, is consistent with the
587 possibility that Sema4B functions in astrocytes as a signaling molecule or a receptor
588 or both. There may, however, be an indirect function in which Sema4B activates a
589 receptor on adjacent cells (other astrocytes or other cell types) after injury, which in
590 turn activates another ligand that can induce astrocyte proliferation. However, the fact
591 that the ectodomains cannot rescue proliferation of mutant astrocytes and have a
592 competitive inhibitor activity on wild-type astrocytes argues strongly for a receptor

type of action. Moreover, the dependence of Sema4B on phosphorylation of a key residue in its intracellular domain for its activity also supports the notion that Sema4B functions as a receptor or a co-receptor in this system. The receptor/ligand for Sema4B has not yet been identified. Since many members of these type 4 semaphorins act via PlexinB1 or B2, it has been suggested that Sema4B might activate one of these receptors (Pasterkamp, 2012). However, because Sema4B phosphorylation can occur downstream to receptor tyrosine kinase signaling, instigated by EGFR, platelet-derived growth factor receptor, or Met (Moritz et al., 2010), it is also possible that in this case Sema4B functions as a signaling molecule in which both binding of the ligand at the extracellular domain and RTK signaling are needed for the activation of signaling downstream of Sema4B.

How does Sema4B function as a signaling molecule?

Our results suggest that the intracellular domain of Sema4B plays a critical role in astrocytes. This intracellular domain contains about 100 amino acids. Except for the COOH-terminal regions, most of this sequence is not conserved within the semaphorin family (although it is quite conserved between species). The COOH-terminal region of Sema4B, as well as of Sema4C, Sema4F and Sema4G, has a PDZ-binding motif (Burkhardt et al., 2005). Sema4B activity in neurons has been suggested to involve PDZ-containing proteins via its PDZ-binding motif (Burkhardt et al., 2005). It is thus possible that one mechanism by which Sema4B interacts with other signaling molecules in astrocytes is through its PDZ-binding motif.

The interacting proteomes in astrocytes are not yet known. Based on a large-scale PDZ-binding selectivity screen across the mouse proteome, it seems that the PDZ-binding domain of Sema4B has the potential to interact with a small number of PDZ-domain proteins, among them the serine proteases HtrA1 and HtrA3 and the

protein phosphatase PTPN13 (Stiffler et al., 2007). Interestingly, Sema4B phosphorylation occurs at serine 825, eight residues from the carboxyl terminal sequence of Sema4B. Phosphorylation of amino acids at this position has been suggested to modulate PDZ-binding functions (Boisguerin et al., 2007). Our data strongly suggest that Sema4B signals to significantly modulate the biology of astrocytes after CNS injury. The detailed regulatory mechanisms of this novel pathway and the impact on the recovery of the CNS after injury remain to be examined.

Citations:

Amankulor NM, Hambardzumyan D, Pyonteck SM, Becher OJ, Joyce JA, Holland EC (2009) Sonic Hedgehog Pathway Activation Is Induced by Acute Brain Injury and Regulated by Injury-Related Inflammation. J Neurosci 29:10299–10308.

Bardehle S, Krüger M, Buggenthin F, Schwausch J, Ninkovic J, Clevers H, Snippert HJ, Theis FJ, Meyer-Luehmann M, Bechmann I, Dimou L, Götz M (2013) Live imaging of astrocyte responses to acute injury reveals selective juxtavascular proliferation. Nat Neurosci 16:580–586.

Boisguerin P, Ay B, Radziwill G, Fritz RD, Moelling K, Volkmer R (2007) Characterization of a Putative Phosphorylation Switch: Adaptation of SPOT Synthesis to Analyze PDZ Domain Regulation Mechanisms. ChemBioChem 8:2302–2307.

Brambilla R, Bracchi-Ricard V, Hu W-H, Frydel B, Bramwell A, Karmally S, Green EJ, Bethea JR (2005) Inhibition of astroglial nuclear factor κB reduces

642 inflammation and improves functional recovery after spinal cord injury. J Exp
643 Med 202:145–156.

644 Burkhardt C, Müller M, Badde A, Garner CC, Gundelfinger ED, Püschel AW (2005)
645 Semaphorin 4B interacts with the post-synaptic density protein PSD-
646 95/SAP90 and is recruited to synapses through a C-terminal PDZ-binding
647 motif. FEBS Lett 579:3821–3828.

648 Bush TG, Puvanachandra N, Horner CH, Polito A, Ostenfeld T, Svendsen CN, Mucke
649 L, Johnson MH, Sofroniew MV (1999) Leukocyte Infiltration, Neuronal
650 Degeneration, and Neurite Outgrowth after Ablation of Scar-Forming,
651 Reactive Astrocytes in Adult Transgenic Mice. Neuron 23:297–308.

652 Cahoy JD, Emery B, Kaushal A, Foo LC, Zamanian JL, Christopherson KS, Xing Y,
653 Lubischer JL, Krieg PA, Krupenko SA, Thompson WJ, Barres BA (2008) A
654 Transcriptome Database for Astrocytes, Neurons, and Oligodendrocytes: A
655 New Resource for Understanding Brain Development and Function. J
656 Neurosci 28:264–278.

657 Codeluppi S, Svensson CI, Hefferan MP, Valencia F, Silldorff MD, Oshiro M,
658 Marsala M, Pasquale EB (2009) The Rheb–mTOR Pathway Is Upregulated in
659 Reactive Astrocytes of the Injured Spinal Cord. J Neurosci 29:1093–1104.

660 Faulkner JR, Herrmann JE, Woo MJ, Tansey KE, Doan NB, Sofroniew MV (2004)
661 Reactive Astrocytes Protect Tissue and Preserve Function after Spinal Cord
662 Injury. J Neurosci 24:2143–2155.

663 Friedel RH, Plump A, Lu X, Spilker K, Jolicoeur C, Wong K, Venkatesh TR, Yaron
664 A, Hynes M, Chen B, Okada A, McConnell SK, Rayburn H, Tessier-Lavigne

M (2005) Gene targeting using a promoterless gene trap vector ("targeted trapping") is an efficient method to mutate a large fraction of genes. Proc Natl Acad Sci U S A 102:13188–13193.

Galou M, Colucci-Guyon E, Ensergueix D, Ridet JL, Ribotta MG y, Privat A, Babinet C, Dupouey P (1996) Disrupted glial fibrillary acidic protein network in astrocytes from vimentin knockout mice. J Cell Biol 133:853–863.

Herrmann JE, Imura T, Song B, Qi J, Ao Y, Nguyen TK, Korsak RA, Takeda K, Akira S, Sofroniew MV (2008) STAT3 is a Critical Regulator of Astrogliosis and Scar Formation after Spinal Cord Injury. J Neurosci 28:7231–7243.

Kindy MS, Bhat AN, Bhat NR (1992) Transient ischemia stimulates glial fibrillary acid protein and vimentin gene expression in the gerbil neocortex, striatum and hippocampus. Brain Res Mol Brain Res 13:199–206.

Liu B, Chen H, Johns TG, Neufeld AH (2006) Epidermal Growth Factor Receptor Activation: An Upstream Signal for Transition of Quiescent Astrocytes into Reactive Astrocytes after Neural Injury. J Neurosci 26:7532–7540.

Lovatt D, Sonnewald U, Waagepetersen HS, Schousboe A, He W, Lin JH-C, Han X, Takano T, Wang S, Sim FJ, Goldman SA, Nedergaard M (2007) The Transcriptome and Metabolic Gene Signature of Protoplasmic Astrocytes in the Adult Murine Cortex. J Neurosci 27:12255–12266.

Maier V, Jolicoeur C, Rayburn H, Takegahara N, Kumanogoh A, Kikutani H, Tessier-Lavigne M, Wurst W, Friedel RH (2011) Semaphorin 4C and 4G are ligands of Plexin-B2 required in cerebellar development. Mol Cell Neurosci 46:419–431.

688 Mandell JW, Gocan NC, Vandenberg SR (2001) Mechanical trauma induces rapid
689 astroglial activation of ERK/MAP kinase: Evidence for a paracrine signal.
690 Glia 34:283–295.

691 Moritz A, Li Y, Guo A, Villen J, Wang Y, MacNeill J, Kornhauser J, Sprott K, Zhou
692 J, Possemato A, Ren JM, Hornbeck P, Cantley LC, Gygi SP, Rush J, Comb
693 MJ (2010) Akt-RSK-S6 Kinase Signaling Networks Activated by Oncogenic
694 Receptor Tyrosine Kinases. Sci Signal 3:ra64.

695 Moussaud S, Draheim HJ (2010) A new method to isolate microglia from adult mice
696 and culture them for an extended period of time. J Neurosci Methods
697 187:243–253.

698 Nakagawa Y, Takamatsu H, Okuno T, Kang S, Nojima S, Kimura T, Kataoka TR,
699 Ikawa M, Toyofuku T, Katayama I, Kumanogoh A (2011) Identification of
700 Semaphorin 4B as a Negative Regulator of Basophil-Mediated Immune
701 Responses. J Immunol 186:2881–2888.

702 Okada S, Nakamura M, Katoh H, Miyao T, Shimazaki T, Ishii K, Yamane J,
703 Yoshimura A, Iwamoto Y, Toyama Y, Okano H (2006) Conditional ablation
704 of Stat3 or Socs3 discloses a dual role for reactive astrocytes after spinal cord
705 injury. Nat Med 12:829–834.

706 Oliva AA, Kang Y, Sanchez-Molano J, Furones C, Atkins CM (2012) STAT3
707 signaling after traumatic brain injury. J Neurochem 120:710–720.

708 Pasterkamp RJ (2012) Getting neural circuits into shape with semaphorins. Nat Rev
709 Neurosci 13:605–618.

Pasterkamp RJ, Verhaagen J (2006) Semaphorins in axon regeneration: developmental guidance molecules gone wrong? Philos Trans R Soc B Biol Sci 361:1499–1511.

Robel S, Berninger B, Götz M (2011) The stem cell potential of glia: lessons from reactive gliosis. Nat Rev Neurosci 12:88–104.

Schildge S, Bohrer C, Beck K, Schachtrup C (2013) Isolation and Culture of Mouse Cortical Astrocytes. J Vis Exp Available at: http://www.jove.com/video/50079/isolation-and-culture-of-mouse-cortical-astrocytes [Accessed November 13, 2013].

Sofroniew MV, Vinters HV (2010) Astrocytes: biology and pathology. Acta Neuropathol (Berl) 119:7–35.

Stiffler MA, Chen JR, Grantcharova VP, Lei Y, Fuchs D, Allen JE, Zaslavskaia LA, MacBeath G (2007) PDZ Domain Binding Selectivity Is Optimized Across the Mouse Proteome. Science 317:364–369.

Toyofuku T, Zhang H, Kumanogoh A, Takegahara N, Yabuki M, Harada K, Hori M, Kikutani H (2004) Guidance of myocardial patterning in cardiac development by Sema6D reverse signalling. Nat Cell Biol 6:1204–1211.

Yamashita K, Vogel P, Fritze K, Back T, Hossmann KA, Wiessner C (1996) Monitoring the temporal and spatial activation pattern of astrocytes in focal cerebral ischemia using in situ hybridization to GFAP mRNA: comparison with sgp-2 and hsp70 mRNA and the effect of glutamate receptor antagonists. Brain Res 735:285–297.

Yang Q, Wang E-Y, Huang X-J, Qu W-S, Zhang L, Xu J-Z, Wang W, Tian D-S (2011) Blocking epidermal growth factor receptor attenuates reactive astrogliosis through inhibiting cell cycle progression and protects against ischemic brain injury in rats. J Neurochem 119:644–653.

Zamanian JL, Xu L, Foo LC, Nouri N, Zhou L, Giffard RG, Barres BA (2012) Genomic Analysis of Reactive Astrogliosis. J Neurosci 32:6391–6410.

Figure legends:

Figure 1: Sema4B is expressed by astrocytes *in vivo*

a. Sema4B-expressing cells were identified in the mouse cortices using anti-β-gal antibody (which recognizes the Sema4B/β-galactosidase (β-gal) fusion protein). In each set of experiments Sema4B$^{+/-}$ mice were analyzed without injury and 1, 3 and 7 days post-injury. A Z-stakes of four optical sections is presented after staining with anti-NeuN, -GFAP, and -β-gal (upper panel) or anti-Iba1, -GFAP, and -β-gal (lower panel). Representative result seven days after injury is shown. Yellow arrows mark examples of astrocytes and orange arrows mark examples of microglia. Note the close proximity of the β-gal staining to the GFAP-positive staining but not to NeuN- or IbaI-positive staining. Scale bars, 10 µM. Multiple cells in a number of sections from three different mice were analyzed at each time point. b. Quantitation of positive cells/section for cells stained with anti-β-gal and -GFAP are shown. c. Immunoblots of protein samples extracted from Sema4B$^{+/+}$ and Sema4B$^{-/-}$ brains are presented. Arrow marks the Sema4B-specific signal and arrowhead marks a non-specific band recognized by this antibody. d. Cortical tissue was dissociated and separated on MACS columns using ACSA-2-beads. Cell samples after separation of cells were

analyzed by FACS using anti-ACSA2-APC antibody. e. Immunoblots of protein samples extracted from the positive ($ACSA2^{+}$) and negative ($ACSA2^{-}$) fractions. The blot was probed with anti-Sema4B antibody. Note that in the positive fraction there are two bands (lower one is the Sema4B signal), while in the negative fraction only the upper band, which is a non-specific band, appears (marked with an arrowhead).

Figure 2: Astrocyte activation profile is modified in $Sema4B^{-/-}$ mutant mice

a. Representative examples of a horizontal section of wild-type (n = 7) and Sema4B mutant cortices were stained with GFAP (green) and Hoechst (blue) seven days after injury. Note reduced activation indicated by GFAP staining near the site of injury in the mutant mouse. Scale bar, 100 µm. b. a representative coronal section of $Sema4B^{+/-}$ with or without injury stained with x-gal histochemistry. Scale bar, 200 µm. The gray boxes mark the area of counting that was used in all sections. c. Quantitation of x-gal-positive cells/area in the non-injured cortex of $Sema4B^{+/-}$ and $Sema4B^{-/-}$ mice. d. Quantitation of x-gal-positive cells/area in the injured cortex of $Sema4B^{+/-}$ and $Sema4B^{-/-}$ mice. e. Representative example of cortex after injury in low magnification, stained with anti-S100β. The black boxes mark the area of counting (in 2f and 2g). Scale bar, 200 µm. Representative example of $Sema4B^{+/-}$ and $Sema4B^{-/-}$ near the site of injury stained with S100β is also shown. Scale bar, 20 µm. Note the typical astrocyte hypertrophy is detected in both $Sema4B^{+/-}$ and $Sema4B^{-/-}$. f. Quantitation of S100 β-positive cells/area in the non-injured cortex of $Sema4B^{+/-}$ and $Sema4B^{-/-}$ mice. g. Quantitation of S100 β-positive cells/area in the injured cortex of $Sema4B^{+/-}$ and $Sema4B^{-/-}$ mice. h., i., j. Relative mRNA levels were measured using real-time PCR analysis (means +/− s.e.m.) of cortical tissue at the site of injury one (i. LCN2, $Sema4B^{+/-}$, n = 4; $Sema4B^{-/-}$, n = 5) and seven (g. GFAP, h. vimentin, n=5) days post-injury ($Sema4B^{+/-}$, n = 5; $Sema4B^{-/-}$, n = 6). *GFAP* LCN-2 and *vimentin* in

each sample were normalized relative to *GAPDH* (similar results were obtained when samples were normalized to ALDH1L1). Note the change in post-injury astrocyte activation profile in the Sema4B$^{-/-}$ cortex (low *GFAP*, normal activation of *vimentin* and higher activation than normal for LCN2. (P values for GFAP p=0.0081 and for LCN2 p=0.0357.

Figure 3: Astrocyte proliferation *in vivo* is reduced in Sema4B$^{-/-}$ mutant mice

a. Representative cortical slices in Sema4B$^{+/+}$ and Sema4B$^{-/-}$ mutant mice seven days post-injury. The panel shows proliferating cells labeled with BrdU (red), activated astrocytes stained with anti-GFAP (green), and total cells labeled with DAPI (blue). Scale bars, 100 µm. b., c. Quantification of total proliferating cells (BrdU^{+}) (b) and of proliferating astrocytes (GFAP^{+}/BrdU^{+}) (c). d. Cell proliferation evaluation by flow cytometry analysis of the cortical injury site. The cortical tissue site was dissociated and analyzed using anti-BrdU and anti-GLAST antibodies. Results in b., c., d. and e. are means +/- s.e.m. b: P =0.032, c: p=0.041 , d: p=0.0285 and e: p=0.0385.

Figure 4: Both acute and chronic inhibition of Sema4B reduce proliferation of astrocytes *in vitro*

a. Sema4B-expressing astrocytes in culture were identified using anti-β-gal antibody and GFAP. Scale bar, 10 µm. b. Quantification of proliferating cultured astrocytes (% Ki-67-positive cells/Hoechst) is shown. For this experiment astrocytes from wild-type and mutant mice were serum-starved for three days before being stimulated with serum and tested for proliferation. c., d. Acute inhibition of Sema4B in primary astrocytes from wild-type mice is shown. c. Representative western blot showing reduction in the levels of Sema4B, 72 h after infection with two different anti-Sema4B shRNAs or a scrambled shRNA (n = 3).. d. Quantification of proliferating shRNA-treated wild-type astrocytes (% Ki-67-positive cells/Hoechst) is shown.

Results in b. and d. are means +/− s.e.m. of four independent experiments in each case. P values for b: $p=2.5^{E-9}$, and for d: p=0.000153 and p=0.000704.

Figure 5: Sema4B is not regulated at the level of mRNA or protein

a., b. Sema4B RNA (a) and protein (b) expression the cortex biopsy near the site of injury. a. Real-time PCR assay of Sema4B mRNA in the cortex at different time points after injury (n = 3). b. Representative western blot of protein samples at different time points after injury are shown (n = 4). c. Protein was extracted from confluent astrocyte cultures at different time points after scratch wound injury and analyzed with anti-Sema4B. The same blots were also tested for tubulin.

Figure 6: Sema4B is phosphorylated at Ser825 after growth factor stimulation or injury

a. Immunoblots of protein samples extracted from $Sema4B^{+/+}$ and $Sema4B^{-/-}$ brains and tested with anti-phospho-Sema4B and anti-tubulin are shown. b. Protein extracted from biopsies of mouse cortical stab-wound injury at different times after injury. Representative result is shown. c. Densitometric analysis of the phospho-Sema4B-to-actin ratio at different times after cortical injury is shown (n = 4). d. Western blots of protein samples were extracted from mouse cortical astrocytes at different times after mechanical injury. Representative western blots obtained with anti-phospho-Sema4B at various time points are shown. The same blots were also tested for p-ERK1/2 and actin. e. Quantification of the phospho-Sema4B-to-actin ratios obtained in the mechanical injury experiments shown (n = 4). f. Western blots of protein samples were extracted from mouse cortical astrocytes at different times after stimulation with 100 ng/ml EGF. g. Densitometric analysis of the phospho-Sema4B-to-actin ratio at different times after stimulation with 100 ng/ml EGF (mean +/− s.e.m. of three

independent experiments is shown for each time point). Results in b., d., and e. are means +/− s.e.m. of four independent experiments.

Figure 7: Sema4B phosphorylation at S825 is critical for its function

a., b. Astrocytes from Sema4B$^{-/-}$ (a) or Sema4B$^{+/-}$ (b) mice were incubated with serum-deficient medium for three days. Astrocytes were then incubated for an additional 16 h with 10% serum and recombinant proteins (50 ng/ml of Fc-only or Sema4B-Fc). Note that Sema4B-Fc was not able to rescue the serum-induced component of Sema4B$^{-/-}$ astrocytes. c., e., f., h., i. Astrocytes isolated from Sema4B$^{+/-}$ or SemaB$^{-/-}$ mutant wild-type mice were infected with lentiviral vectors expressing empty vector, wild-type (full-length) Sema4B, or point mutations that abolish Sema4B phosphorylation. Astrocytes were selected with blasticidin until all non-infected astrocytes died. c. Western blots of protein samples extracted from the infected astrocytes and tested for myc tag expression is shown. d., g. HEK293 cells transfected with PlexinA1 tagged with myc at the intracellular domain with (g) or without detergent (d) is shown. Scale bars, 20 µm. e., f., h., i. Representative astrocytes infected with the different vectors and stained with anti-myc tag in the absence of detergent are also shown. Scale bars, 10 µm. j., k. Sema4B$^{-/-}$ (j) and Sema4B$^{+/-}$ (j, k) astrocytes infected with the different Sema4B mutants were incubated in serum-deficient medium for three days before being stimulated for 16 h with 10% serum. Their proliferation was monitored by expressing Ki-67-positive astrocytes as a fraction of the total number of astrocytes in the same fields. Results are means +/− s.e.m. of four independent experiments. P values for b p= 0.0247, for j p=0.0247.

Table 1: Post-hoc power calculations for *m* independent experiments with

Bonferroni correction *k*

From Fisher's chi-square test for combined probabilities, we have that x^2 (df=2*m*) ~ –2ln(p1p2…pm), where pi is the p-value for the ith independent experiment. The post-hoc Expected Value of x^2 is just the degrees of freedom (df) + the noncentrality parameter (λ). Thus, for 3 independent experiments, say λ is given by –2ln(p1p2p3) – 6. The power can then be obtained directly using G*Power 3 software with α = 0.05/k.

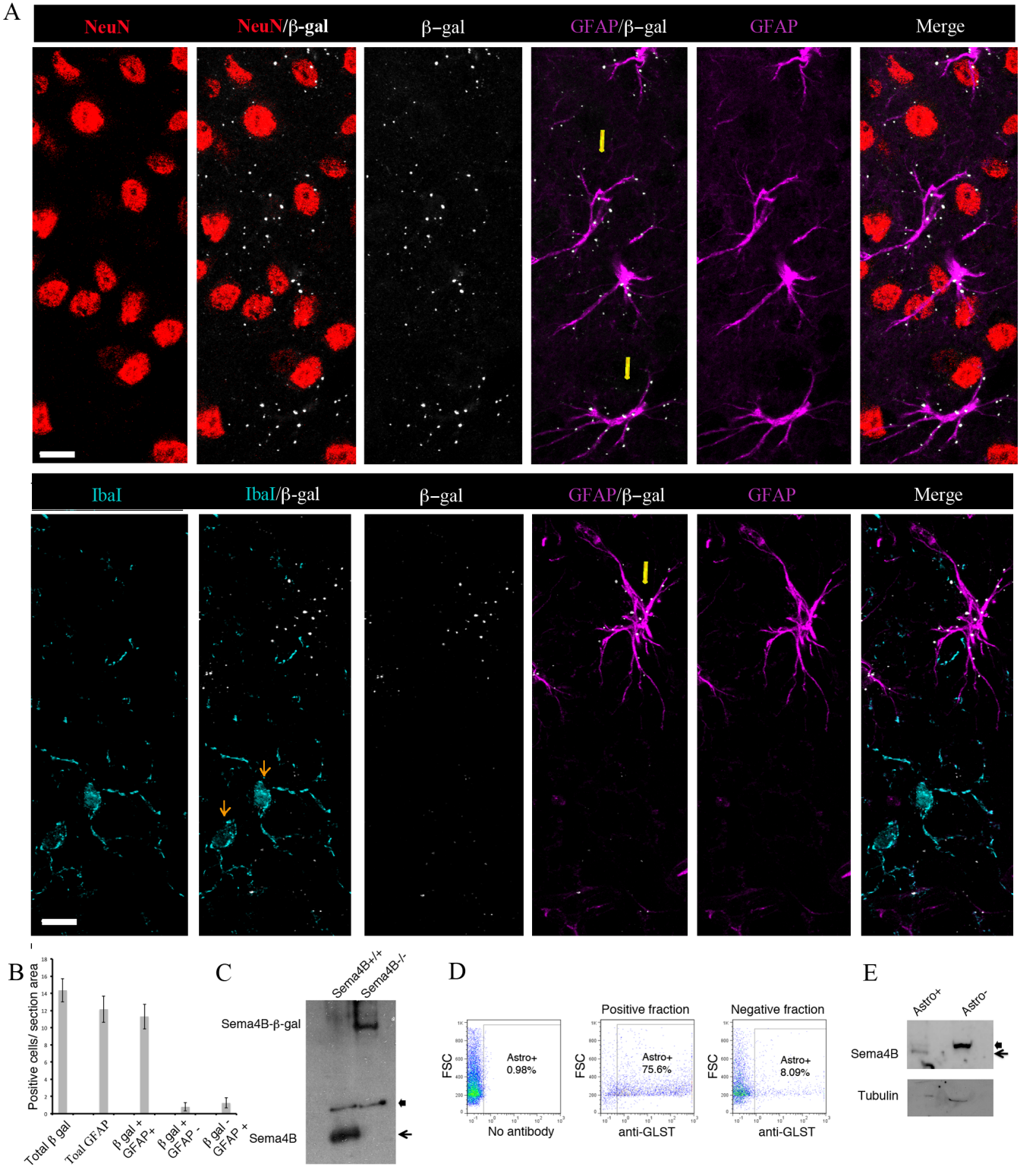

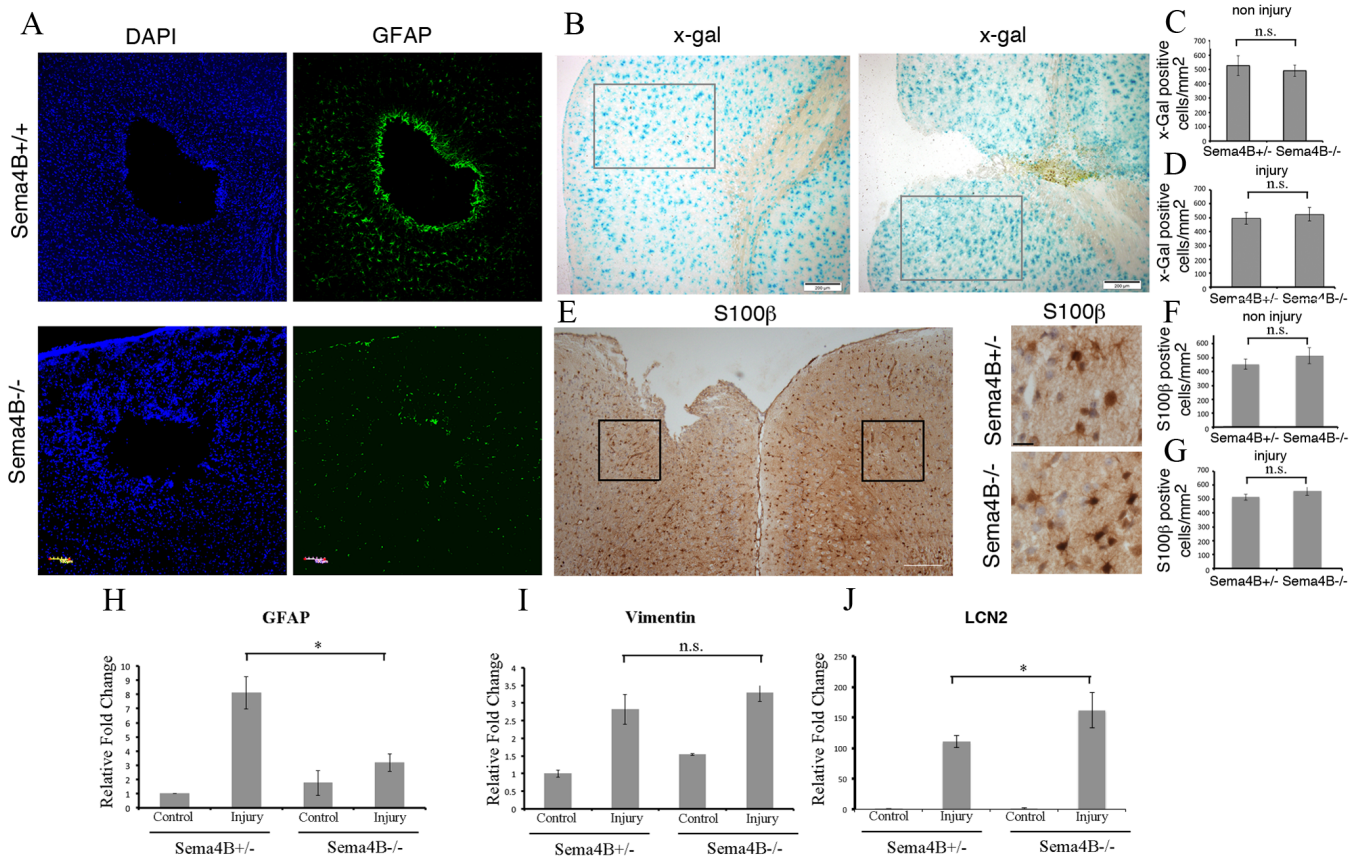

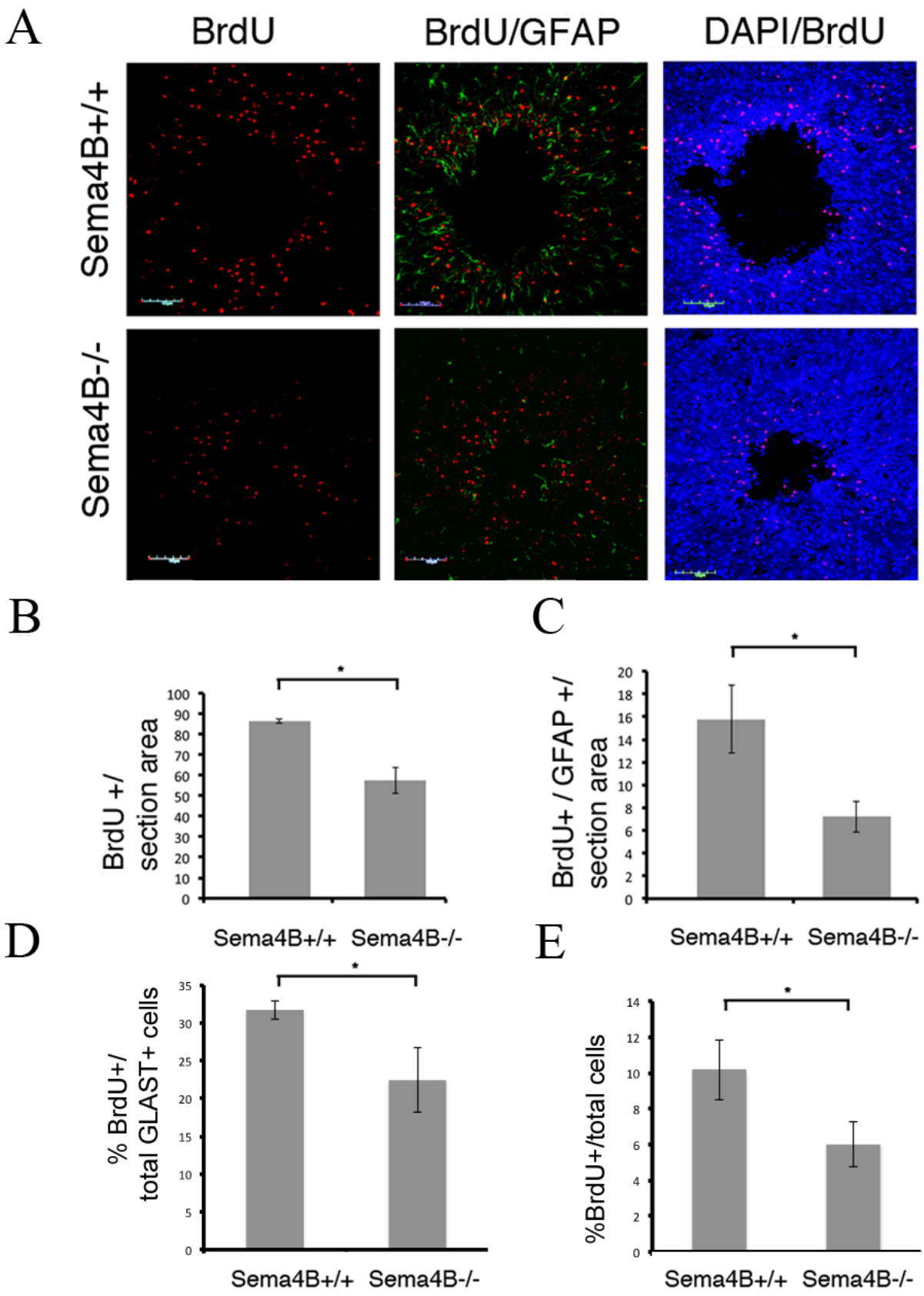

A

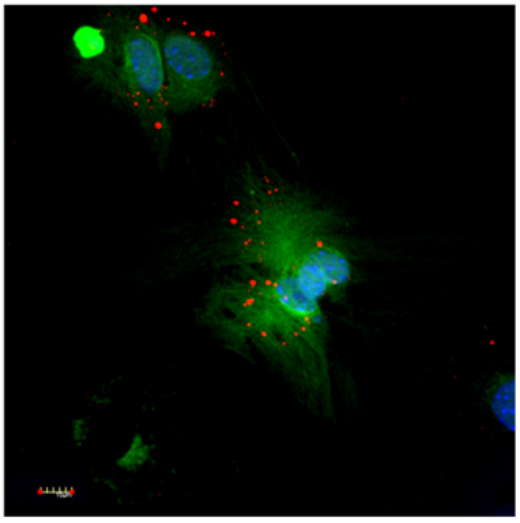

B

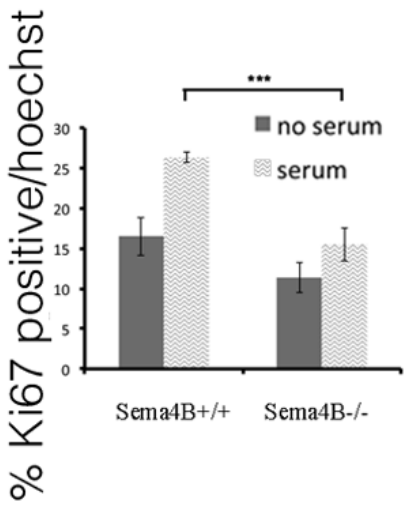

C

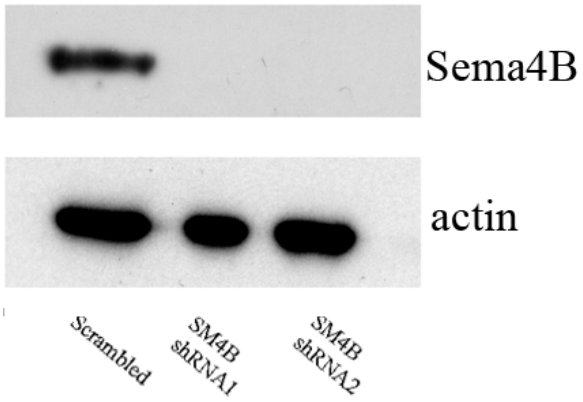

D

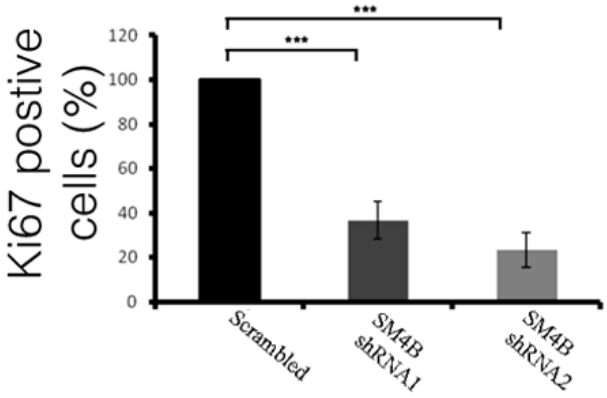

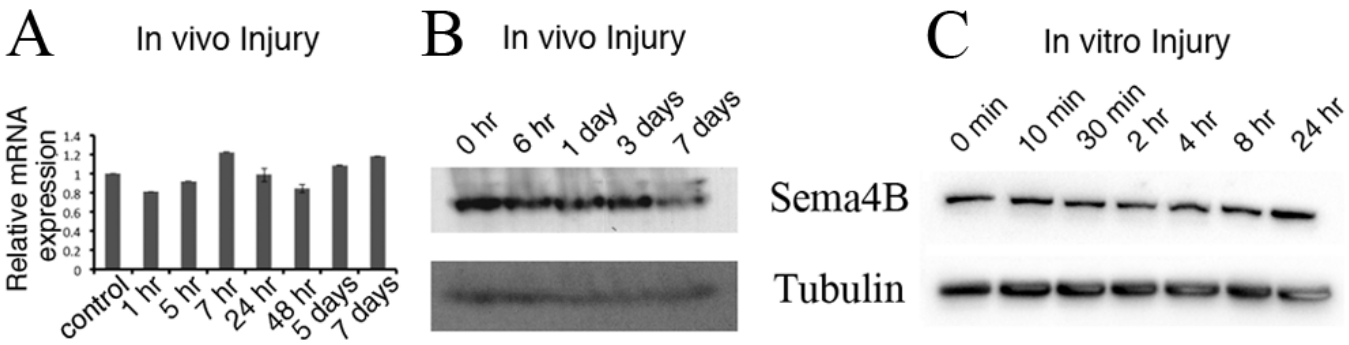

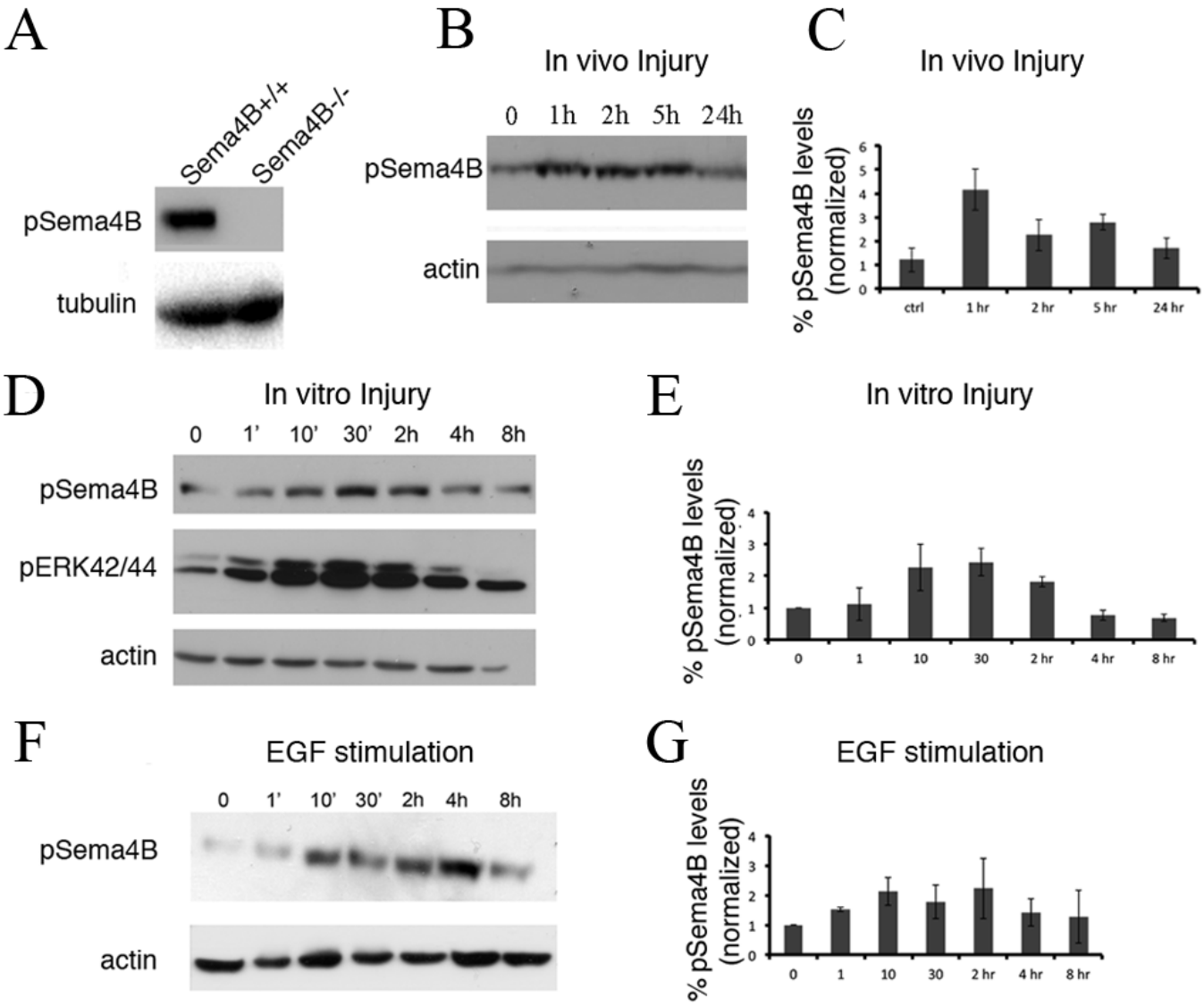

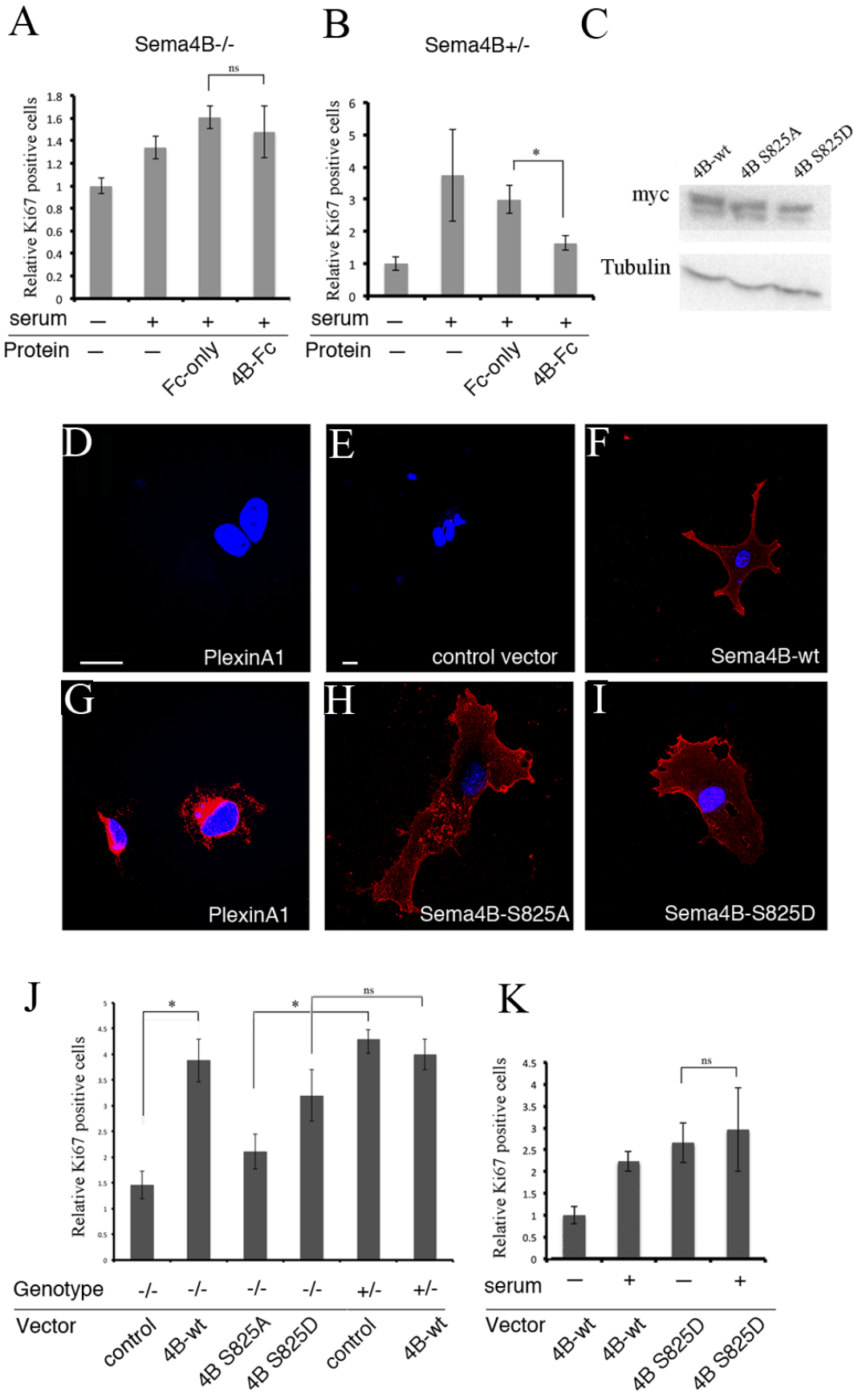

figure		***Data structure***	***Type of test***	***Power***
2	c	Normality not assumed	Mann-Whitney	55.9
	d	Normality not assumed	Mann-Whitney	53.2
	f	Normality not assumed	Mann-Whitney	61.7
	g	Normality not assumed	Mann-Whitney	10.7
	h	Normality not assumed	Mann-Whitney	12.3
	i	Normality not assumed	Mann-Whitney	2.6
	j	Normality not assumed	Mann-Whitney	12.6
3	b	Normality not assumed	Mann-Whitney	21.5
	c	Normality not assumed	Mann-Whitney	63.3
	d	Normality not assumed	Mann-Whitney	36.4
4	b	Normality not assumed	Mann-Whitney	100
	d	Normality not assumed	Mann-Whitney	100 100
7	a	Normality not assumed	Mann-Whitney	37.1
	b	Normality not assumed	Mann-Whitney	90
	j	Normality not assumed	Mann-Whitney	100 100
	k	Normality not assumed	Mann-Whitney	99.9 100